THE JOURNAL OF PHYSICAL CHEMISTRY C

ARTICLE

pubs.acs.org/JPCC

Site-Specific CO_2 Adsorption and Zero Thermal Expansion in an Anisotropic Pore Network

Wendy L. Queen,[†,‡] Craig M. Brown,[*,†,§] David K. Britt,[∥] Pawel Zajdel,[⊥] Matthew R. Hudson,[†,‡] and Omar M. Yaghi[*,∥]

[†]NIST Center For Neutron Research, 100 Bureau Drive, Gaithersburg Maryland 20899-6102, United States

[‡]Department of Materials Science and Engineering, University of Maryland, College Park, Maryland 20742, United States

[§]The Bragg Institute, Australian Nuclear Science and Technology Organisation, PMB1, Menai, NSW, Australia

[∥]Department of Chemistry and Biochemistry, University of California, Los Angeles, California 90095, United States

[⊥]Division of Physics of Crystals, Institute of Physics, University of Silesia, ul. Uniwersytecka 4, 40-007 Katowice, Poland

Supporting Information

ABSTRACT: Detailed neutron powder diffraction (NPD) experiments were carried out on the parent and CO_2 adsorbed Mg-MOF-74 (MOF: metal−organic framework). Data collected at low temperature revealed two CO_2 adsorption sites on the pore surface and multiple changes in the framework as a function of CO_2 loading. Upon heating the samples to room temperature, the data revealed minimal changes in expansivity upon adsorption of up to 0.94 CO_2/Mg (≈ 25% mass fraction). Further, temperature-dependent data collected on the bare framework reveals net zero thermal expansion between 10 and 475 K.

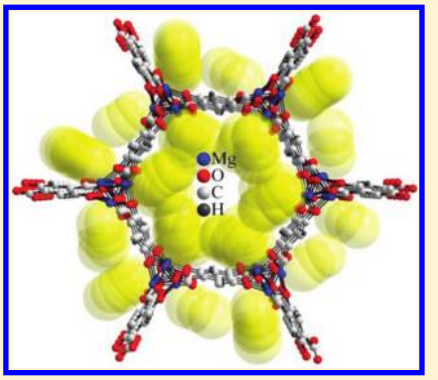

INTRODUCTION

Separation of CO_2 from flue gas streams and other point sources is an important component in the mitigation of atmospheric CO_2. While methods exist to separate CO_2 from the other components of a postcombustion stream (primarily scrubbing with liquid amine solutions), their wide implementation on an industrial scale has not been possible due to the massive energy requirement of such processes.[1] Efficient methods for effecting such a separation are urgently sought. Metal−organic frameworks (MOFs) are a versatile class of compounds with a nearly infinite number of building block combinations. Their high internal surface areas coupled with chemical tunability make them particularly attractive for the selective capture of CO_2.[2−5] Recent work has shown that the incorporation of coordinatively unsaturated metal centers (UMCs) into the frameworks provide enhanced binding energy and an increase in surface packing density of adsorbates due to the highly reactive, electron deficient nature of the sites.[6−18] While UMCs provide strong interactions allowing CO_2 adsorption close to room temperature and slightly above, these interactions are weak relative to the formation of chemical bonds also providing facile CO_2 release during regeneration processes.

The activated MOF-74 series of compounds are candidates for selective adsorption of CO_2, having unsaturated 5-coordinate metal ions decorating the inside of one-dimensional hexagonal channels. Of these, the Mg-MOF-74 material was recently found to exhibit an exceptionally high CO_2 uptake at low pressure (<0.1 bar) and room temperature and easy, reversible adsorption/desorption of CO_2.[19,20] In order to obtain a better understanding of how structure dictates function during adsorption/desorption processes, we have performed detailed neutron diffraction experiments, allowing us to probe structural changes in the framework as well as the exact positions, occupancy, and site affinity of the gas as it is adsorbed. These studies have for the first time allowed the identification of a secondary CO_2 adsorption site. Comparisons between the bare and CO_2-adsorbed phase reveal no significant change in the unit cell volume for room temperature CO_2 adsorption, a property that might be of particular interest for the future implementation of adsorbent materials in separation/storage applications. Further, temperature-dependent studies performed on the bare framework have revealed a net zero thermal expansion (ZTE) over a wide range of temperatures, a phenomenon that to the best of our knowledge has not before been reported in a highly porous MOF system.

Received: September 4, 2011
Revised: November 7, 2011
Published: November 08, 2011

ACS Publications © 2011 American Chemical Society

Table 1. Unit Cell Parameters, CO_2 Occupancies, and Selected Bond Distances and Angles of Mg-MOF-74 (Trigonal, R-3).[a]

CO_2 per Mg site	0	0.25	0.5	0.75	1.0	1.75
temperature (K)	20	20	20	20	20	20
distances (Å)						
Mg−O(2b)	-----	2.39(6)	2.34(3)	2.30(2)	2.28(3)	2.24(3)
O(2a)−C(2a)	-----	1.1(1)	1.07(5)	1.17(3)	1.13(4)	1.14(3)
O(2b)−C(2a)	-----	1.04(9)	1.06(4)	1.06(2)	1.10(3)	1.06(3)
O(3a)−C(3a)	-----	-----	-----	-----	1.23(7)	1.12(3)
O(3b)−C(3a)	-----	-----	-----	-----	1.2(1)	1.10(2)
C(2a)−O(2)		3.10(8)	3.10(3)	3.19(2)	3.35(2)	3.46(3)
C(2a)−C(3)		3.07(9)	3.09(4)	3.21(2)	3.16(3)	3.20(3)
C(3a)−O(2)	-----	-----	-----	-----	3.1(1)	3.23(3)
C(3a)−O(3)	-----	-----	-----	-----	3.07(9)	3.27(3)
angles (°)						
O(2a)−C(2a)−O(2b)	-----	150(15)	164(6)	172(4)	167(4)	170(3)
Mg−O(2b)−C(2a)	-----	125(7)	128(3)	129(2)	134(2)	144(2)
O(3a)-C(3a)-O(3a)	-----	-----	-----	-----	177(1)	178(2)
unit cell parameters						
a (Å)	25.921(2)	25.895(2)	25.867(1)	25.847(2)	25.824(1)	25.767(1)
c (Å)	6.8625(8)	6.8705(6)	6.8768(7)	6.8788(6)	6.8904(5)	6.9145(5)
volume ($Å^3$)	3993.5(5)	3989.7(5)	3984.8(4)	3979.8(5)	3979.4(3)	3975.8(3)
occupancy of CO_2						
site I	0	0.24(1)	0.60(1)	0.89(1)	0.88(1)	0.99(1)
site II	0	0	0	0	0.24(1)	0.86(2)

[a] The values in parentheses represent one standard deviation.

RESULTS AND DISCUSSION

Rietveld refinement[21] of the neutron powder diffraction (NPD) data obtained from bare Mg-MOF-74 is well described using a structural model similar to that published.[22] After structural refinement of the host material, Fourier difference maps allowed subsequent elucidation of CO_2 site positions that were further refined along with their occupancies as a function of loading. Development of a suitable structural model permitted nearly unconstrained Rietveld refinements (see Supporting Information).

The lowest loading, at 0.25 CO_2/Mg, reveals that the CO_2 only populates a single site, I, located at the UMC. As shown in Table 1, the refined site I occupancy is in good agreement with this initial CO_2 loading. The Mg−O(2b)−C(2a) interaction exhibits a highly angular orientation, 125(7)°, with two short lateral interactions, approximately 3.1 Å, between the electron deficient C(2a) of the CO_2 molecule, and the framework atoms, O(2) and C(3) (Figure 1, left). The gas molecule exhibits an "end on" coordination (Figure 1, right), similar to that reported in an X-ray analysis of CO_2 in Ni-MOF-74.[23] The Mg−O(2b) distance is relatively short at 2.39(6) Å, consistent with the reported high initial isosteric heat of adsorption (−47 kJ/mol[22,24] and −39 kJ/mol[19]). As observed previously[23] the interaction between the framework and CO_2 and the local potential that it sits in gives rise to an unexpected nonlinear geometry of the gas molecule with a refined intramolecular angle of significantly less than 180°. The next closest CO_2/framework distance (∼2.9 Å) is found between O(2b) and O(2), which is equatorially coordinated to the Mg^{2+} ion. This distance, only slightly shorter than the sum of the van der Waals radii for two O atoms[25] (3.04 Å) is likely a limiting factor in the approach of the CO_2 molecule to the framework surface as electrostatic repulsion would begin to destabilize the CO_2 adsorption. The observed atomic displacement parameters (ADP) for C(2a) and O(2a) (0.06(2) $Å^2$ and 0.12(2) $Å^2$, respectively) are rather large compared to those of the framework atoms and the Mg bound O(2b). One interpretation is that the large binding energy present between Mg and O(2b) leads to a strong localization on the position of the binding oxygen, whereas the remaining CO_2 atoms have weaker interaction with the framework and are less constrained, creating a distribution of positions and an "apparent" bending that is likely static in nature. This argument is further supported by density functional theory (DFT) calculations, which show the lowest energy rotational/vibrational mode for CO_2 adsorbed in Mg-MOF-74 to be ∼4.3 meV.[26] This mode is only likely to be thermally populated at the 10% level for our lowest measurement temperature of 20 K.

As the loading level is increased, the refinements progress in a systematic fashion; however, at 1.0 CO_2/Mg the first sign of population of the second site, II, occurs. Increasing the loading to 1.75 CO_2/Mg leads to an even greater increase in site II occupancy (0.86(2)) and large ADPs for the oxygen associated with this additional molecule. Both oxygen atoms were refined anisotropically, improving the refinement, and the resulting displacement ellipsoids appear to be elongated (Figure 1, right). Although it is unclear as to whether the origin of the elongation is static or dynamic in nature, it is more likely that at 20 K, it is due to slight differences in CO_2 orientation within the channel rather than thermal motion of the molecules. The weak van der Waals interaction between the CO_2 and framework could lead to a rather flat local potential and a lack in orientation preference upon adsorption. Attempts to model the site II CO_2 as two discrete molecular units with slightly rotated orientations are possible, but require a highly constrained molecular structure, leading us to prefer the anisotropic ADP description. Our observation of population at site II contradicts the assertions made by Wu et. al[26]

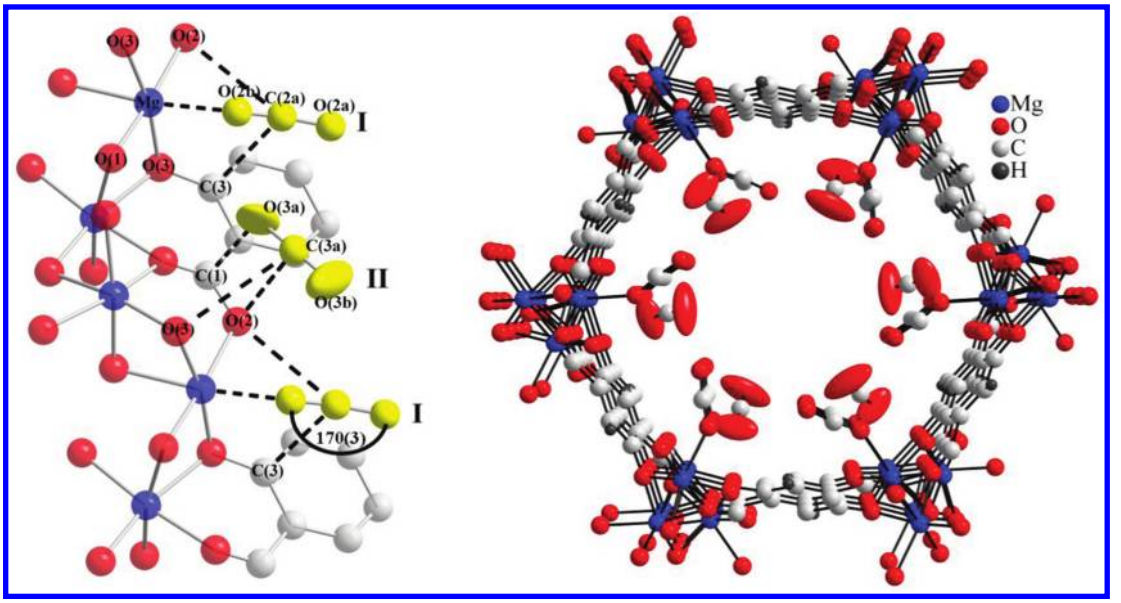

Figure 1. (left) Close up view of Mg-MOF-74 loaded with 1.75 CO_2 (yellow) per Mg showing the nearest neighbor interactions found between the CO_2 sites (I and II) and the framework. These are shown as dashed black lines, the longest of which is ~3.47 Å. (right) Ball and stick model of Mg-MOF-74 loaded with 1.75 CO_2 per Mg (viewed along the crystallographic *c* axis). The figure reveals two crystallographically distinct CO_2 adsorption sites. The second CO_2 site was refined anisotropically to illustrate the disorder found in the nuclear density. The thermal ellipsoids are drawn at 50% probability.

who assumed that secondary adsorption sites would not be associated with the framework surface due to the packing density of site I; however, recent adsorption studies have indicated population of this site is likely to occur at room temperature and even at low-pressure.[27]

The CO_2 orientation in II is not parallel with that of I, but instead is canted between two site I molecules allowing full surface coverage. Although the exact intermolecular distances are susceptible to uncertainties in site II, due to disordered O(3a,b), there is an average intermolecular distance of approximately 3 Å. Further, there appears to be strong interactions along the pore-channel direction, allowing multiple site II/framework interactions (Figure 1, left). These distances, which range from ~3 Å to 3.25 Å, indicate that the binding enthalpy associated with II is significantly lower than that for I. Additionally, observed similarities between intermolecular distances and site II CO_2/framework distances, all of which are comparable to the sum of the van der Waals radii for C (1.70 Å) and O (1.52 Å), indicate that the site II CO_2 has a similar strength of interactions with nearest neighbor gas molecules as with the framework.

Systematic increases in the amount of loaded gas reveals several trends in the structural response to CO_2 adsorption in Mg-MOF-74 (Table 1). First, the Mg−O(2b) distance decreases over the entire loading range from ~2.39 Å to ~2.24 Å. These distances are comparable to what has been observed in the previously reported study of the Ni-MOF-74 analogue at 2.29(2) Å.[23] Additionally, despite the fact that NPD data has been collected on CO_2-loaded Mg-MOF-74 previously, the report lacks further structural information, and the loading dependence was unevaluated.[26] The second structural response to CO_2 loading is an overall decrease in the unit cell volumes. Despite a slight expansion in the *c* axis at higher CO_2 loadings, the volume reduction stems from a significant reduction along the *a*- and *b*-axes (Figure 2). Our results are contrary to a recent report by Valenzano et al., who use theoretical calculations to estimate structural features of the Mg-MOF-74 framework upon CO_2

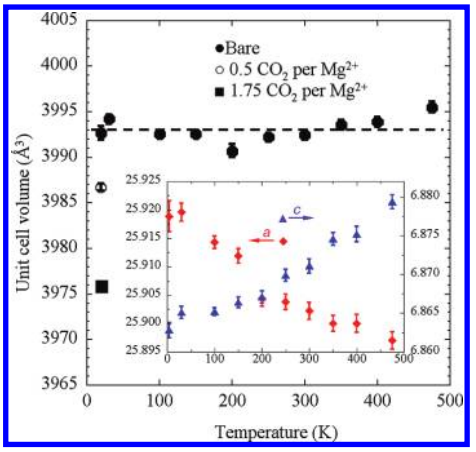

Figure 2. Plot showing unit cell volume of the bare Mg-MOF-74 as a function of temperature. As a reference, the volumes of Mg-MOF-74 at 20 K loaded with 0.5 and 1.75 CO_2 per Mg are shown. The dashed line represents the average unit cell volume. The inset shows the increase in the *a*/*b*-axes and a simultaneous decrease in the *c*-axis of the bare material upon increasing temperature. The error bars represent one standard deviation, sometimes being smaller than the symbol size.

adsorption.[24] Their study shows a slight lengthening of the average Mg−O distances in the MgO_5 moeity and a 1% increase in unit cell volume, both of which they assert is due to a slight displacement of the Mg cation from the framework. Our observed volume reduction can be rationalized when looking at the O(1,2,3)−Mg−O(2b) angles (Figure 1, left). Upon increasing the loading level, these angles show a gradual increase from an average value of 87.8° at 0.25 to 90.6° at 1.75 CO_2/Mg. This implies that increased repulsive interactions between the electronegative O atoms as the Mg and CO_2 molecule become closer induce a compression of the *a*- and *b*-axes, creating an overall decrease in the unit cell volumes from 3993.4(5) $Å^3$ for the parent material to

dx.doi.org/10.1021/jp208529p |*J. Phys. Chem. C* 2011, 115, 24915–24919

3975.9(4) Å^3 for the 1.75 CO_2/Mg loading, a change of −0.44%. It should be noted that the observed changes in the Mg−O(1,2,3)−O(2b) angles allow preservation of O(2b)−O(1,2,3) distances, which range from 3.04 to 3.08 Å, throughout our five loadings. The third trend involves a steady increase in the Mg−O(2b)−C(2a) angle, which ranges from 125(7)° to 129(2)° until there is significant occupancy of site II, after which it jumps to 144(2)°. This trend is presumably related to slight changes in packing energetics of CO_2 in the pore. As Mg−O(2b) and intermolecular CO_2−CO_2 interactions increase, there is a subsequent decrease in van der Waals site I CO_2/framework interactions, which is substantiated by a lengthening of the C(2a)−O(2) distance from ∼3.1−3.2 Å for 0.25−0.75 loadings to ∼3.35 Å and 3.46 Å for the 1.0 and 1.75 loadings, respectively.

It has been noted in several studies that CO_2 coordination at the UMC in MOF-74 derivatives leads to the unexpected nonlinear geometry of the adsorbed molecule.[23,26] There are several phenomena that could contribute to the appearance of such a behavior, including (1) an actual bending due to direct charge transfer between the UMC and site I CO_2; (2) static disorder in the positions of C(2a) and O(2a), a direct result of weak interactions between these atoms and framework walls; and (3) phonon-induced dynamic disorder resulting from an asymmetric wagging motion. A recent study by Wu et al. reports frozen phonon calculations of CO_2 adsorbed Mg showing a minimal energy penalty for deviations of up to 10° (<less than 25 meV/molecule) from the normal linear geometry of a free CO_2 molecule.[26] When taking into account the strong Mg−CO_2 interaction, indicated by short Mg−O(2b) distances and large enthalpy for adsorption, it is therefore expected at low-temperatures that angles ≤170° must have some contribution from static disorder resulting in a misinterpretation of the actual bond angle from refinement of the time- and position-averaged diffraction data. In the present study, refined O(2a)−C(2a)−O(2b) angles in the 20 K data are within error of the expected 170° bond angle, except for the lowest loading, which likely has the largest amount of disorder. After performing several experiments on this material, our experience indicates that fast cooling/rapid adsorption can lead to a distribution of adsorption amounts/locations throughout the sample. Rietveld refinement of these nonequilibrated samples lead to larger apparent error in the refined parameters and a larger apparent bending of the CO_2 molecule. With quench cooling of CO_2 in Mg-MOF-74, the refined models show bond angles of 160° with unphysical ADPs that necessitate restraining their values to being equal and positive. The data we show here, however, result in excellent goodness-of-fit parameters with unrestrained model refinement that lead to more reasonable intramolecular angles and ADPs that get progressively larger on traversing the CO_2 atoms away from the Mg^{2+} ion. However, even in the case of the lowest loading at 20 K, the adsorption is so rapid it is effectively quenched, and we observe a much smaller intramolecular angle similar to that previously published.[23,26]

Given the intrinsic limitations of Fourier difference techniques and atom-based Rietveld analysis, we additionally turned to the maximum entropy method (MEM)[28] to reconstruct the scattering densities (Figure S3−S7, Supporting Information), removing model-bias from our approach and further confirming the shape of the adsorbed CO_2 molecule. While conventional diffraction studies are based on an atomistic model, and thermal motion or static disorder are usually accounted for in terms of split positions and/or anisotropic ADPs, MEM can offer increased freedom from the atomic approximation. In the case of Mg-MOF-74, MEM was applied in visualizing the scattering density of adsorbed CO_2 molecules for two data sets with nominal 0.5 and 1.75 CO_2/Mg loadings (data measured at 20 K). Even though the atom positions are much more evident from the extracted nuclear densities compared to Fourier techniques (Supporting Information), we conclude that there is no improvement in describing the data when applying an MEM approach compared to Rietveld analysis, and that Mg-MOF-74 is adequately described using the atomic model.

After collecting 20 K NPD data on the sample loaded with 0.5 and 1.75 CO_2/Mg, the temperature was increased to 300 K, and the data was collected again. The 0.5 loading showed no significant change in the site I CO_2 occupancy (0.63(2)) upon heating, while for the 1.75 loading, site II was completely evacuated, and site I maintained a relatively high CO_2 occupancy equal to 0.94(3). These results again reiterate that the high initial isosteric heat of adsorption for Mg-MOF-74 is directly related to the UMC. The physisorptive nature of this interaction is further evidenced by the lengthening of the Mg−O(2b) bond with increased temperature: 2.48(5) Å and 2.58(5) Å for the 0.5 and 1.75 (300 K), respectively. The unit cell volumes of the 0.5 and 1.5 loadings at 300 K (3992.3(5) Å^3 and 3992.0(5) Å^3, respectively) are comparable to the volume of the bare material, indicating that occupancy of site I at room temperature has little effect on the overall unit cell volume. In fact, the volume is constant from the bare to loaded phase within ∼0.06% error (±1.5 Å^3). Despite the lack of volume change, the room temperature data still shows a similar compression of *a*/*b* and simultaneous expansion of *c* with higher loading as observed for the framework at 20 K data.

For further comparison, temperature-dependent NPD studies were carried out on the bare framework. Rietveld refinement of the data revealed unusual thermal behavior. While most materials undergo thermal expansion in all three-dimensions upon heating, Mg-MOF-74 instead undergoes compression along the *a*/*b* axes and a simultaneous expansion along *c*. This structural response leads to an approximate ZTE over a fairly wide range of temperatures, 20−475 K (Figure 2), quite different from the usual negative thermal expansion (NTE) seen in cyanides, MOF-5, HKUST-1, and COF-102,[29−33] although ZTE has been observed in cubic cyanides.[34] The current NPD data does not allow a clear determination of the mechanism for the observed thermal properties, as the changes in the overall unit cell are minimal. Further, much of the NTE reported in MOFs thus far has been attributed to dynamic properties related to low-energy vibrational modes of various rigid units found within the frameworks,[31,32] but similar efforts have not yet been made for MOF-74.

CONCLUSION

We have performed a detailed structural analysis of Mg-MOF-74 while systematically increasing temperature and the amount of adsorbed CO_2. We have observed the first structural evidence of population of a second CO_2 adsorption site associated with the framework and speculate that even further CO_2 adsorption would be forced to form a second layer, as current intermolecular distances will not permit any further adsorption directly onto the framework surface. In contrast to other published data that report larger deviations from the normal linear geometry, a careful experimental approach and application of bias-free MEM analysis provides confidence in a model resulting in a more realistic bond angle of approximately 170° in all cases.

■ ASSOCIATED CONTENT

Supporting Information. Detailed experimental procedures, neutron powder diffraction patterns, additional structural images, and crystallographic information are provided as Supporting Information. This material is available free of charge via the Internet at http://pubs.acs.org.

■ AUTHOR INFORMATION

Corresponding Author

*(C.M.B.) E-mail: craig.brown@nist.gov; phone: (301) 975-5134; fax: (301) 921-9847. (O.M.Y.) E-mail: yaghi@chem.ucla.edu; phone: (310) 206-0398; fax: (310) 206-5891.

■ ACKNOWLEDGMENT

W.Q. gratefully acknowledges the NIST NRC postdoctoral research associateship program.

■ REFERENCES

(1) Kohl, A. L.; Nielsen, R. B. *Gas Purification*; 5th ed.; Gulf Publishing Company: Houston, TX, 1997.
(2) Millward, A. R.; Yaghi, O. M. *J. Am. Chem. Soc.* **2005**, *127*, 17998–17999.
(3) Thallapally, P. K.; Tian, J.; Radha Kishan, M.; Fernandez, C. A.; Dalgarno, S. J.; McGrail, P. B.; Warren, J. E.; Atwood, J. L. *J. Am. Chem. Soc.* **2008**, *130*, 16842–16843.
(4) Finsy, V.; Ma, L.; Alaerts, L.; De Vos, D.; Baron, G.; Denayer, J. *Microporous Mesoporous Mater.* **2009**, *120*, 221–227.
(5) Demessence, A.; D'Alessandro, D. M.; Foo, M. L.; Long, J. R. *J. Am. Chem. Soc.* **2009**, *131*, 8784–8786.
(6) Chen, B.; Ockwig, N. W.; Millward, A. R.; Contreras, D. S.; Yaghi, O. M. *Angew. Chem., Int. Ed.* **2005**, *44*, 4745–4749.
(7) Roswell, J. L. C.; Yaghi, O. M. *Angew. Chem., Int. Ed.* **2005**, *44*, 4670–4679.
(8) Wong-Foy, A. G.; Matzger, A. J.; Yaghi, O. M. *J. Am. Chem. Soc.* **2006**, *128*, 3494–3495.
(9) Dincă, M.; Dailly, A.; Liu, Y.; Brown, C. M.; Neumann, D. A.; Long, J. R. *J. Am. Chem. Soc.* **2006**, *128*, 16876–16883.
(10) Collins, D. J.; Zhou, H. *J. Mater. Chem.* **2007**, *17*, 3154–3160.
(11) Dincă, M.; Han, W.; Liu, Y.; Dailly, A.; Brown, C.; Long, J. *Angew. Chem., Int. Ed.* **2007**, *46*, 1419–1422.
(12) Britt, D.; Tranchemontagne, D.; Yaghi, O. M. *Proc. Natl. Acad. Sci. U.S.A.* **2008**, *105*, 11623–11627.
(13) Dincă, M.; Long, J. R. *Angew. Chem., Int. Ed.* **2008**, *47*, 6766–6779.
(14) Liu, Y.; Kabbour, H.; Brown, C. M.; Neumann, D. A.; Ahn, C. C. *Langmuir* **2008**, *24*, 4772–4777.
(15) Yan, Y.; Lin, X.; Yang, S.; Blake, A. J.; Dailly, A.; Champness, N. R.; Hubberstey, P.; Schröder, M. *Chem. Commun.* **2009**, 1025–1027.
(16) Wu, H.; Zhou, W.; Yildirim, T. *J. Am. Chem. Soc.* **2009**, *131*, 4995–5000.
(17) Ma, S.; Yuan, D.; Chang, J.; Zhou, H. *Inorg. Chem.* **2009**, *48*, 5398–5402.
(18) Yan, Y.; Telepeni, I.; Yang, S.; Lin, X.; Kockelmann, W.; Dailly, A.; Blake, A. J.; Lewis, W.; Walker, G. S.; Allan, D. R.; Barnett, S. A.; Champness, N. R.; Schröder, M. *J. Am. Chem. Soc.* **2010**, *132*, 4092–4094.
(19) Britt, D. K.; Furukawa, H.; Wang, B.; Glover, T. G.; Yaghi, O. M. *Proc. Nat. Acad. Sci. U.S.A.* **2009**, *106*, 20637–20640.
(20) Yazaydin, A. O.; Snurr, R. Q.; Park, T.-H; Koh, K.; Liu, J.; LeVan, M. D.; Benin, A. I.; Jakubczak, P.; Lanuza, M.; Galloway, D. B.; Low, J. J.; Willis, R. R. *J. Am. Chem. Soc.* **2009**, *131*, 18198–18199.
(21) Toby, B. H. *J. Appl. Crystallogr.* **2001**, *34*, 210–213.
(22) Caskey, S. R.; Wong-Foy, A. G.; Matzger, A. J. *J. Am. Chem. Soc.* **2008**, *130*, 10870–10871.
(23) Dietzel, P. D. C.; Johnsen, R. E.; Fjellvag, H.; Bordiga, S.; Groppo, E.; Chavan, S.; Blom, R. *Chem. Commun.* **2008**, 5125–5127.
(24) Valenzano, L.; Civalleri, B.; Chavan, S.; Palomino, G. T.; Areán, C. O.; Bordiga, S. *J. Phys. Chem. C* **2010**, *114*, 11185–11191.
(25) Bondi, A. *J. Phys. Chem.* **1964**, *68*, 441–451.
(26) Wu, H.; Simmons, J. M.; Gadiapelli, S.; Zhou, W.; Yildirim, T. *Phys. Chem. Lett.* **2010**, *1*, 1946–1951.
(27) Mason, J. A.; Sumida, K.; Herm, Z. R.; Krishna, R.; Long, J. R. *Energy Environ. Sci.* **2011**, *4*, 3030–3040.
(28) Gilmore, C. J. *Acta Crystallogr.* **1996**, *A52*, 561–589.
(29) Goodwin, A. L.; Kepert, C. J. *Phys. Rev. B* **2005**, *71*, 140301−1–140301−4.
(30) Chapman, K. W.; Chupas, P. J.; Kepert, C. J. *J. Am. Chem. Soc.* **2006**, *128*, 7009–7014.
(31) Zhou, W.; Wu, H. *Phys. Rev. B* **2008**, *78*, 054114-1–054114-5.
(32) Wu, Y.; Kobayashi, A.; Halder, G. J.; Peterson, V. K.; Chapman, K. W.; Lock, N.; Southon, P. D.; Kepert, C. J. *Angew. Chem., Int. Ed.* **2008**, *47*, 8929–8932.
(33) Zhao, L.; Chongli, Z. *J. Phys. Chem. C* **2009**, *113*, 16860–16862.
(34) Phillips, A. E.; Halder, G. J.; Chapman, K. W.; Goodwin, A. L.; Kepert, C. J. *J. Am. Chem. Soc.* **2010**, *132*, 10–11.